Nickel functionalized mesostructured cellular foam (MCF) silica as a catalyst for solventless deoxygenation of palmitic acid to produce diesel-like hydrocarbons

Lilis Hermida[1,2], **Ahmad Zuhairi Abdullah**[1,*] and **Abdul Rahman Mohamed**[1]

[1] School of Chemical Engineering, Universiti Sains Malaysia, 14300 Nibong Tebal, Penang, Malaysia
[2] Department of Chemical Engineering, Universitas Lampung, Bandar Lampung 35145, Lampung, Indonesia
*E-mail: chzuhairi@eng.usm.my *Tel: +604-594 1013

Mesostructured cellular foam (MCF) silicas synthesized at different conditions were incorporated with nickel to synthesize nickel functionalized MCF catalysts. Morphologies of the MCF silicas and the catalysts were characterized using nitrogen adsorption-desorption, scanning electron microscope (SEM) and energy dispersive X-ray (EDX). Activities of the catalysts were evaluated based on solventless deoxygenation of palmitic acid for 6 h at 300 ^{o}C under inert atmosphere in a semi batch reactor for production of n-pentadecane and 1-pentadecene as hydrocarbon fuels. Palmitic acid conversion of 86.4% with n-pentadecane selectivity of 31.8 % and 1-pentadecene selectivity of 29.2 % was achieved by a catalyst using TEOS amount of 9.2 ml and aging time of 3 days in the MCF syntheses. The highest activity of the catalyst was attributed to the highest nickel content together with the smallest nickel particles dispersed in the catalyst.

Keywords: mesostructured cellular foam; silica; nickel incorporation; deoxygenation; palmitic acid; hydrocarbon fuels.

1. Introduction

Diesel fuel demand is predicted to grow from 24 million barrels per day in 2009 to 34 million barrels per day by 2030 as reported in OPEC World Oil Outlook [1]. Diesel fuel is derived from fossil fuel source which is non-renewable and the amount is finite. Therefore, the increasing demand of diesel fuel leads to an important development of biomass-based technologies to produce biofuels. Biomass, a renewable source, is biological material from living organisms such as, trees, crops, animals, plants, co-product from industrial process and wastes from agriculture and industries [2]. Biomass supplies are not limited since trees, animals and crops are biologically reproducible and waste will always exist.

Palm fatty acid distillate (PFAD) is a co-product of the physical refining of crude palm oil (CPO) to produce refined, bleached and deodorized (RBD) palm oil in which CPO is obtained from oil palm fruits through an oil mill, as can be seen in Fig. 1. The RBD palm oil is usually used for production of vegetable oil and can also be used in the manufacture of margarine, shortening, ice cream and condensed milk [3]. PFAD contains more than 90 % palmitic acid [4]. So far, PFAD is mostly used as a raw material for laundry soap industries [4]. The use of PFAD as feedstock for production of biofuels, as value-added products, has more advantages in terms of price and availability, especially in Malaysia and Indonesia, as these countries are the world's top-two largest CPO producers [4,5].

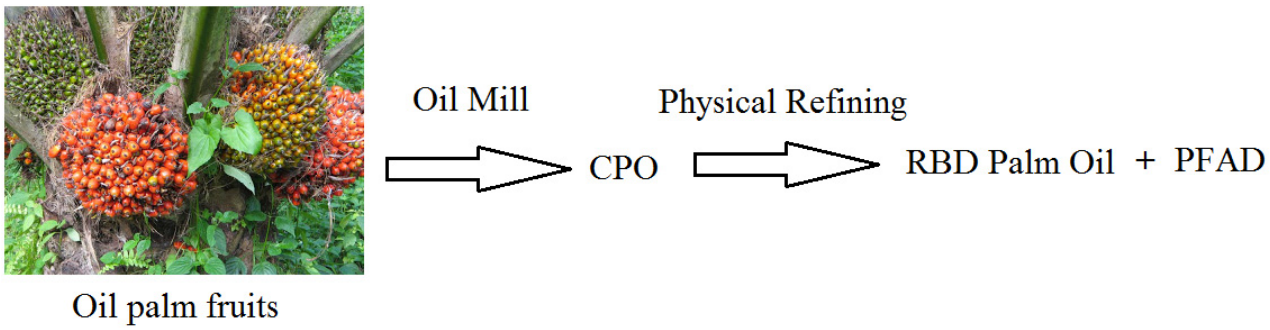

Fig. 1 Palm fatty acid distillate (PFAD) as a co-product of physical refining process of CPO to RBD palm oil

Production of biofuels from various renewable feedstocks has been extensively studied for many years. Transesterification of vegetable oil with methanol is commonly used for production of biodiesel which is a prominent biofuel. Biodiesel contains fatty acid methyl esters (FAMEs) and is usually used in a mixture with diesel fuel [6]. Next-generation biofuel could be diesel like-hydrocarbons produced by catalytic deoxygenation of fatty acids over metal supported catalysts. The catalytic deoxygenation of fatty acids is a potential technology that generates linear corresponding n-alkanes (parafins) and alkenes (olefins) through decarboxylation and decarbonilation [7], respectively, as can be seen in Fig. 2. Meanwhile, CO_2 and CO are formed as gaseous products. The n-alkanes and alkenes are

hydrocarbons that are similar to those found in diesel fuel derived from fossil fuel resources, for example n-heptadecane and 1-heptadecene from stearic acid deoxygenation, n-pentadecane and 1-pentadecene from palmitic acid deoxygenation, etc. [8]. As such, the diesel like-hydrocarbons can be directly used and fully compatible with existing diesel engines without modification.

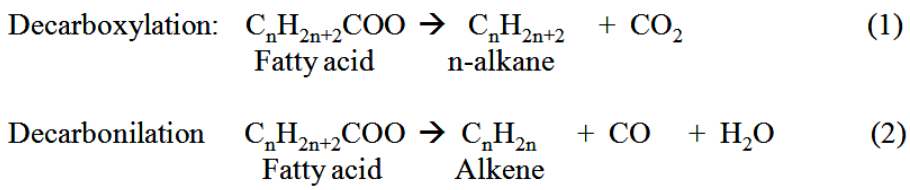

Fig. 2. Deoxygenation of fatty acid through decarboxylation and decarbonilation

Deoxygenation of steric acid and palmitic acid over several active metals such as Pd supported on various supports (silica, activated carbon and mesoporous carbon Sibunit) have been successfully carried out at 300 ^{o}C [9.10]. Due to the high price of Pd, researchers has also investigated several catalysts with different active sites (hydrotacites and nickel) and different supports (MgO/Al_2O_3 and Al_2O_3), as alternative catalysts [11-14]. A series of hydrotalcite catalysts with different ratios of magnesium oxide to alumina (MgO/Al_2O_3) have been investigated for deoxygenation of oleic acid at 300-400 ^{o}C. Subsequantly, deoxygenation of triolein over Ni supported on alumina (Al_2O_3) catalysts has been studied at 350 ^{o}C. However, the process generated various types of hydrocarbon fuels such as heptanes, octane, nonane and heptadecane due to the occurrence of cracking reaction during the deoxygenation. Besides due to the application of higher temperatures, this could be due to small pore diameters (below 20 Å) of the alumina (Al_2O_3) based catalysts. According to the literatures, the effective catalysts having mesopore sizes (20 – 500 Å) are required for reactions involving bulky molecules such as fatty acid to diminish diffusion limitation of reactants and products during the reaction [15-17].

Mesostructured cellular foam (MCF) is a class of three-dimensional (3D) hydrothermally robust materials with ultra-large pore size (up to 500 Å) [18]. Owing to their larger pore sizes, MCF materials have advantages in terms of better diffusion of reactants and products. However, there has been limited information about the utilization of MCF silica as supports for loading of catalytically active component. Therefore, in the present study catalyst made from various MCF silicas have been incorporated with inexpensive metal i.e. nickel for deoxygenation of palmitic acid, as a representative of PFAD, to produce diesel-like hydrocarbons i.e. n-pentadecane and 1-pentadecene.

2. Experimental

2.1 Preparation of MCF silica supports

Various MCF silica support materials were prepared according to a previously reported procedure [19] with modification in terms of the tetraethyl ortho silicates (TEOS) amount (from 9.2 to 35 ml) and aging time (from 1 to 3 days), as given in Table 1. In a typical synthesis, 4 g of Pluronics 123 (P123) was dissolved in 70 ml of 1.6 M HCl. Then, 3.4 ml of trimethylbenzene (TMB) was added, and the resulting solution was heated to 40 ^{o}C with rapid stirring to synthesize a microemulsion (template). After stirring for 2 h, TEOS (*T*) was added to the solution and stirred for 5 min. Then, the solution was transferred into a poly-ethylene bottle and kept at 40 ^{o}C in an oven for 20 h for formation of pre-condensed silica foam. After that, the mixture was removed from the oven and then NH_4F.HF (46 mg in 5 ml of deionised water) was added to the mixture with slow mixing. Then, it was aged at 80 ^{o}C in an oven for certain duration (*D*). After cooling, the mixture was filtered and then dried at 100 ^{o}C for 12 h. After that, calcination was carried out in static air at 300 ^{o}C for 0.5 h and 500 ^{o}C for 6 h to remove the template. Hereafter, the synthesis materials will be donated as MCF (*a*T-*b*D), where *a* is the amount of TEOS and *b* is duration of aging time.

Table 1 Modification used in the synthesis of MCF silica support materials

No	Supports	Amount of TEOS (T), ml	Aging time (D), day
1	MCF(9.2T-2D)	9.2	2
2	MCF(12.5T-2D)	12.5	2
3	MCF(16T-2D)	16	2
4	MCF(9.2T-1D)	9.2	1
5	MCF(9.2T-3D)	9.2	3

2.2 Incorporation of nickel (Ni) into MCF silica materials

The MCF silica supports were functionalized with nickel using a deposition-precipitation method adopted from literature [20]. In the procedure, 250 ml of an aqueous solution containing 10.156 g of $Ni(NO_3)_2.6H_2O$ and 0.3 ml of HNO_3 69 % wt/wt was prepared. In a typical preparation, 40 ml of the aqueous solution was used for dissolving 6.3 g of urea at room temperature to make a urea solution and 210 ml of the aqueous solution was mixed with 1.9 g of the MCF support to make a suspension. The suspension was heated at 40 ^oC, and then mixed with the urea solution under rapid mixing. After that, the mixture was heated to 90 ^oC for 2 h under static condition. After cooling, the mixture was filtered and the solid was washed three times with 20 ml of hot distilled water (~50 ^oC) followed by drying at 100 ^oC for 12 h. Then, the solids were calcined in static air at 300 ^oC for 6 h. Then the calcined samples were reduced at 550 ^oC for 2.5 h under hydrogen stream, and then cooled to room temperature in nitrogen flow to obtain nickel functionalized MCF catalysts. The catalysts are designated NiMCF(aT-bD)(R) in which *a* is the amount of TEOS and *b* is duration of aging time in the synthesis of MCF supports, as given in Table 2.

Table 2 Modification used in the synthesis of MCF silica materials

No	Supports	Catalysts
1	MCF(9.2T-2D)	NiMCF(9.2T-2D)(R)
2	MCF(12.5T-2D)	NiMCF(12.5T-2D)(R)
3	MCF(16T-2D)	NiMCF(16T-2D)(R)
4	MCF(9.2T-1D)	NiMCF(9.2T-1D)(R)
5	MCF(9.2T-3D)	NiMCF(9.2T-3D)(R)

2.3 Characterization

Nitrogen adsorption-desorption isotherm data were obtained using a Quanta-chrome Autosorb 1C automated gas sorption analyzer operated at liquid nitrogen temperature to estimate average cell pore size, average window pore size, specific pore volume and specific surface area (S_{BET}). Average cell pore size was evaluated using Barrett-Joyner-Halenda (BJH) method from the adsorption branch of the isotherm data. Meanwhile, average window pore size was evaluated using BJH method from the desorption branch. S_{BET} was calculated using Brunauer-Emmett-Teller (BET) method. Samples were also analyzed using Leo Supra 50 VP field emission scanning electron microscope (SEM), equipped with an Oxford INCAX act, energy dispersive X-ray (EDX) microanalysis system, to obtain SEM images and chemical compositions. Prior to the analysis, samples were mounted on stubs with double-sided adhesive tape. Then, the samples were coated with high purity gold and observed at room temperature.

2.4 Solventless deoxygenation of palmitic acid

Solventless deoxygenation of palmitic acid was performed in a semibatch mode in which CO_2 and CO gases produced during the reaction was continuously removed. The deoxygenation was carried out in a 250 mL three-necked flask reactor equipped with a magnetic stirring bar, reflux condenser and a tube to pass pure nitrogen flow to reaction mixture. During the deoxygenation reaction, the nitrogen stream swept the evolved gases through the condenser and a trap containing 50 ml of 1 M sodium hydroxide. The reactor was placed on a hot plate.

Palmitic acid (4.5 g) and catalyst (0.45 g) were first added into the reactor. Before the reaction was started, nitrogen flow was passed through the reaction mixture for about 30 min. Then, the reaction mixture was heated to 300 ^oC and maintained for 6 h to perform deoxygenation of palmitic acid without solvent under rapid stirring and nitrogen flow. The liquid product was collected and analyzed by means of an Agilent Technology 7890A GC system equipped with a flame ionization detector and a non-polar capillary column (GsBP-5). Palmitic acid conversion was calculated based on the amount of palmitic acid converted in the reaction divided by initial number of moles of palmitic acid loaded into the reactor. The selectivity was calculated as the number of moles of product recovered divided by the number of moles of palmitic acid that had reacted.

3. Results and discussion

3.1 Characterization of nickel functionalized MCF catalysts

Schematic cross section of MCF silica as reported in the literature is of strut-like structure as given in Fig. 3, which shows that the cells of the MCF structure are framed by the silica struts [18]. The disordered array of silica struts are composed of uniform-sized spherical cells interconnected by window pores. Surface characteristics of MCF materials prepared with different TEOS amounts and aging times and the corresponding nickel functionalized MFC catalyst using nitrogen adsorption-desorption can be seen in Table 3.

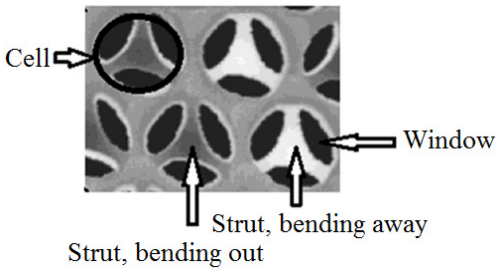

Fig. 3. Schematic cross section of MCF silica adopted from adopted from Schmidt-Winkel *et al* [18]

Table 3 Surface characteristics of MCF materials and corresponding nickel functionalized MCF catalysts

Supports	S_{BET}, m^2/g	V_{pore}, cm^3/g	d_{cell}, Å	d_{window}, Å	Catalysts	S_{BET}, m^2/g	V_{pore}, cm^3/g	d_{cell}, Å	d_{window}, Å
MCF(9.2T-2D)	375	2.24	232	130	NiMCF(9.2T-2D)(R)	281	1.02	184	125
MCF(12.5T-2D)	404	1.62	231	102	NiMCF(12.5T-2D)(R)	324	1.05	230	100
MCF(16T-2D)	336	1.41	235	102	NiMCF(16T-2D)(R)	309	0.92	235	100
MCF(9.2T-1D)	394	1.85	235	125	NiMCF(9.2T-1D)(R)	253	0.93	233	153
MCF(9.2T-3D)	378	2.12	235	158	NiMCF(9.2T-3D)(R)	307	1.09	234	90

d_{cell} and d_{window} pore are the cell and window pore diameters, respectively, determined using the BJH method,
S_{BET} is the surface area determined based on the BET method, and
V_{pore} is the total pore volume determined at a relative pressure of 0.9948

When using the same aging time (2 days) in the MCF support synthesis, the increase in TEOS amount from 9.2 ml to 12.5 ml resulted in an increase in total surface area of the MCF silica material. However, its pore volume, cell size and window pore size decreased to suggest that the thicknesses of the MCF walls increased. Further increase in TEOS amount from 12.5 ml to 16 ml was found to decrease the total surface area and the pore volume. Meanwhile, the cell size increased but the window pore size was virtually unchanged. The main reason for the above phenomenon was attributed to a higher number TMB/P123 microemulsion phase that interacted with protonated silicate species leading to the formation of the 'soft silica"–coated TMB/P123 microemulsion phase. Then, condensation of silica in the walls led to a higher the formation of Si-O-Si linkages in the form of mesostructure in the MCF. Meanwhile, the use of an extra TEOS amount in the synthesis interrupted the condensation of silica network. This resulted in a detrimental effect to the formation of mesostructure in the MCF [21]. This behaviour was similar to that in the synthesis of SBA-15 silica materials [22].

For the use of the same TEOS amount (9.2 ml), window pore size in MCF silica supports increased with increasing aging time whilst cell size remained stable, as suggested by data in Table 3. This result could be attributed to the 'soft silica"–coated TMB/P123 composite droplets that experienced an increase in size and consequently expanded the window pore size. At the same time, condensation of silica in the walls took place with the formation of Si-O-Si linkages to solidify the inorganic network, and subsequently the materials with increased pore size gradually rigidified [18, 21]. As longer aging duration was allowed, the larger window pore size in MCF structure would be obtained. As a result, the highest window pore size (158 Å) was achieved at aging time of 3 days as longest aging duration in the synthesis of MCF supports.

Deposition-precipitation method generally involves the conversion of a highly soluble metal precursor into another substance which specifically precipitates onto a support and not in the solution [23]. Incorporation of nickel into MCF silica supports using deposition-precipitation method resulted in some changes in textural parameters such as total surface area, total pore volume, cell size and window pore size, as can be seen in Table 3. Mechanism of nickel incorporation into MCF silica has been previously reported [24]. The mechanism was assumed to be analogous to nickel incorporation into Spherosil as reported in the literature [25]. It is suggested that the changes in the textural parameters were affected by the partial dissolution of siliceous pore and by the deposition of nickel particles [25]. Table 3 generally shows that incorporation of nickel into MCF supports resulted in decreases in total surface area, pore volume, cell size and window pore size due to deposition of nickels. However, for MCF(9.2T-1D) support prepared at TEOS amount of 9.2 ml and an aging time of 1 day, the window pore size increased from 125 Å to 153 Å after the incorporation of nickel. This behaviour was most likely due to a greater consumption of the siliceous pore walls during the deposition-precipitation [24].

All nitrogen adsorption-desorption isotherm curves, as shown in Fig. 4, are of type IV characterized by hysteresis in multilayer range of physisorption isotherms, which is often associated with capillary condensation (the pore filling process) in mesopore structure [26]. The functionalization of MCF supports with nickel resulted in a reduction in the

nitrogen adsorption-desorption isotherm curves of nickel functionalized MCF catalysts. However, the forms of the curves did not appreciably change after functionalization with nickel. This observation indicated that total pore volume experienced a decrease but the mesoporosity of the MCF materials was maintained after they were incorporated with nickel as suggested in the literature [27]. Mesoporosity are pores with diameter between 20 and 500 Å [26]. The results were in agreement with the surface characteristic results in Table 3 in which all nickel functionalized MCF catalysts had window pore sizes (from 90 to 153 Å) in the range of mesoporosity. Window pores are gates for reactants access to the cell where the active centres were mostly located in the catalysts [28]. The mesoporosity of catalysts is needed for reactions involving bulky molecules of fatty acids to reduce diffusion limitations faced by reactants and products within the catalyst pores during the process to consequently increase the their activities [15-17].

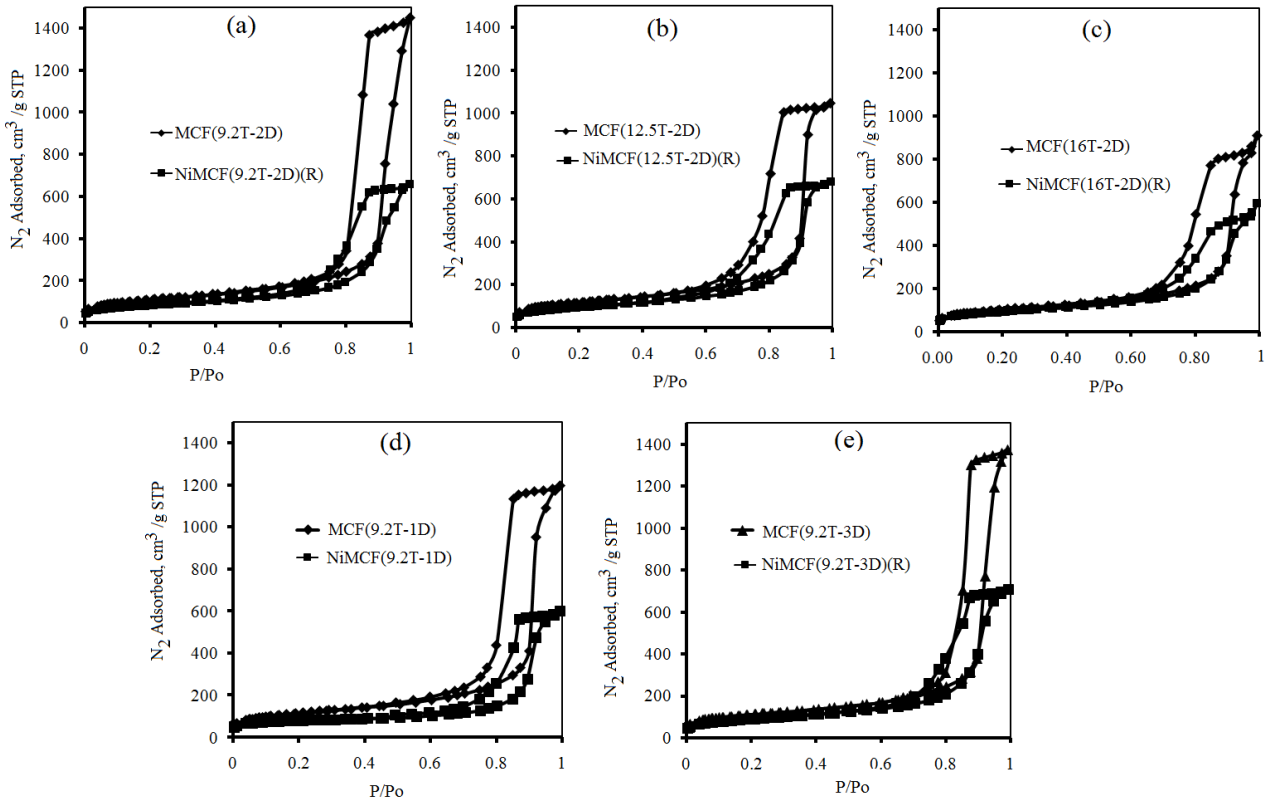

Fig. 4 Nitrogen adsorption-desorption isotherm of (a): MCF(9.2T-2D) support and NiMCF(9.2T-2D)(R) catalyst, (b): MCF(12.5T-2D) support and NiMCF(12.5T-2D)(R) catalyst, (c): MCF(16T-2D) support and NiMCF(16T-2D)(R) catalyst, (d): MCF(9.2T-1D) support and NiMCF(9.2T-1D)(R) catalyst, (e): MCF(9.2T-3D) support and NiMCF(9.2T-3D)(R) catalyst.

Morphologies of nickel functionalized MCF catalysts were examined using SEM. The results are shown in Fig. 5. The morphology of the nickel functionalized MCF catalysts was strongly influenced by the structural characteristics of the supports. For catalysts using MCF supports prepared at the same aging time (2 days), the increase in TEOS amount resulted in thicker and larger sizes of nickel particles to present in the catalysts. At TEOS amount of 9.2 in the MCF synthesis, uniform nickel nanoparticles in the form of nanoworms were observed in NiMCF(9.2T-2D)(R) catalyst. Meanwhile, nickel particles in the form of layered and platelet structures were observed in NiMCF(9.2T-2D)(R) and NiMCF(9.2T-2D)(R) catalysts using MCF supports prepared at TEOS amount of 12.5 ml and 16 ml, respectively. This result was attributed to a higher density of silanol groups (Si-OH) in the MCF support. As such, more $Ni(OH)_2(OH_2)_4$ complex reacted with the silanol groups in the MCF supports during the deposition-precipitation process to increase the nickel particle sizes, as suggested in the literature [24, 29]. Meanwhile, for catalysts using the same TEOS amount (9.2 ml) in the MCF syntheses, sizes of nickel particles present in the catalysts slightly decreased with the increase in aging time. Nickel nanoparticles in the form of nanoworms dispersed in NiMCF(9.2T-1D)(R) catalyst prepared using MCF support with an aging time of 1 day were slightly larger compared to those in NiMCF(9.2T-2D)(R) and NiMCF(9.2T-3D)(R) catalysts prepared using MCF support at aging times of 2 and 3 days, respectively.

Chemical compositions of the catalysts were determined using EDX, as can be seen in Fig. 6. NiMCF(9.2T-2D)(R) catalyst using MCF support prepared at TEOS amount of 9.2 ml was found to contain metallic nickel 5.3 wt. % with the same aging time (2 days) in the MCF synthesis. When the TEOS amount was increased from 9.2 ml to 12.5 ml, the metallic nickel content in the catalyst decreased to 3.1 wt. %. These observations suggested that the use of TEOS amount of 9.2 ml in the MCF synthesis led to homogeneous distribution of nickel inside and outside the cells in

NiMCF-9.2T(R) catalyst. This can be confirmed by the surface characteristic results in Table 3 where the deposition of the MCF(9.2T-2D) support with nickel resulted in higher reductions in cell size from 232 to 184 Å and in window pore size from 130 to 125 Å. Meanwhile, the use of TEOS amount of 12.5 ml in the MCF synthesis resulted in NiMCF(12.5T-2D)(R) catalysts with metallic nickel in the form of layered and platelet structures that could be mainly distributed outside the cells in the catalysts. However, further increase in TEOS amount from 12.5 to 16 ml resulted in NiMCF(16T-2D)(R) with a higher content of metallic nickel (14.1 wt. %) due to larger and thicker sizes of metallic nickel particles which were in the form of layered and platelet structures. Surface characteristic results in Table 3 confirm that there were no appreciable changes in cell sizes of MCF(12.5T-2D) and MCF(16T-2D) after the nickel incorporation, which suggested that the metallic nickel particles were mainly located outside the cells.

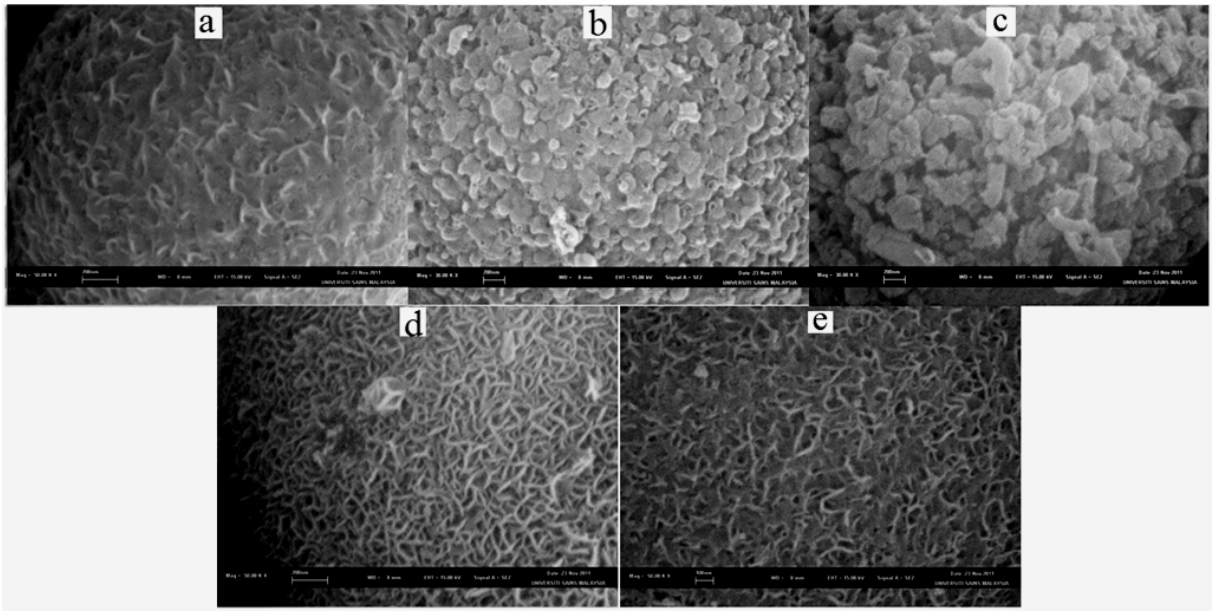

Fig. 5 SEM images of (a): NiMCF(9.2T-2D)(R), (b): NiMCF(12.5T-2D)(R), (c): NiMCF(16T-2D)(R), (d): NiMCF(9.2T-1D)(R) and (e): NiMCF(9.2T-3D)(R) catalysts.

Furthermore, at the same TEOS amount (9.2 ml) in the MCF support syntheses, the increase in aging time was found to increase the amount of nickel compositions present in the catalyst, as can be seen in Fig. 6. The highest amount of nickel was found to be 17.57 wt. % in the NiMCF(9.2T-3D(R) catalyst that used MCF support prepared at the longest aging time (3 days). It was envisioned that window pore size of MCF material used as a support was the main factor that influenced the nickel nanoparticle incorporation. The window pore size of MCF support prepared using an aging time of 3 days (MCF(9.2T-3D)) support was the highest among them. Then, window pore size of MCF(9.2T-2D) was higher than that of MCF(9.2T-1D), as presented in Table 3. As such, most of nickel nanoparticles were easily introduced through the window pore size of MCF(9.2T-3D) support. It can be concluded in this study that larger window pore size of MCF support resulted in easier incorporation of nickel nanoparticles with smaller sizes. Hence, a suitable support was necessary for obtaining a high dispersion of nickel species with small sizes.

3.2 Solventless deoxygenation of palmitic acid over nickel functionalized MCF catalysts

Catalytic performances of nickel functionalized MCF catalysts with different surface characteristics and nickel compositions were evaluated for deoxygenation of palmitic acid at 300 ^{o}C in solvent free condition under nitrogen flow for 6 h in a semi batch mode. Conversions of palmitic acid and selectivities of desirable products (n-pentadecane and 1-pentadecane) recorded during the experimental runs are shown in Table 4. NiMCF(9.2T-2D)(R) catalyst exhibited a higher palmitic acid conversion of 59 % compared to NiMCF(12.5T-2D)(R) and NiMCF(16T-2D)(R) catalysts using MCF support prepared at an aging time of 2 days. The higher palmitic acid conversion exhibited by NiMCF(9.2T-2D)(R) catalyst was attributed to small nickel nanoparticles dispersed in the catalyst, albeit it had the second highest nickel content among the catalysts using MCF support prepared at aging time of 2 days, as confirmed from SEM and EDX results in Fig. 5 and Fig. 6, respectively. Meanwhile, for the same MCF preparation in terms of TEOS amount (9.2 ml), NiMCF(9.2T-3D)(R) achieved the conversion of 86.4 % which was the highest active catalyst. Besides the small nickel nanoparticles dispersed in NiMCF(9.2T-3D)(R) catalyst, this was due to the highest nickel content, i.e 17.57 wt. %, in the catalyst, as confirmed in EDX results in Fig. 6. Metallic nickel species were active sites to produce n-alkane and alkene in fatty acid deoxygenation through decarboxylation and decarbonilation reaction [12]. It is also reported in

the literature that for most metal supported catalysts, smaller active metal particles dispersed in the support may also lead to the higher catalytic activity in the reaction [30].

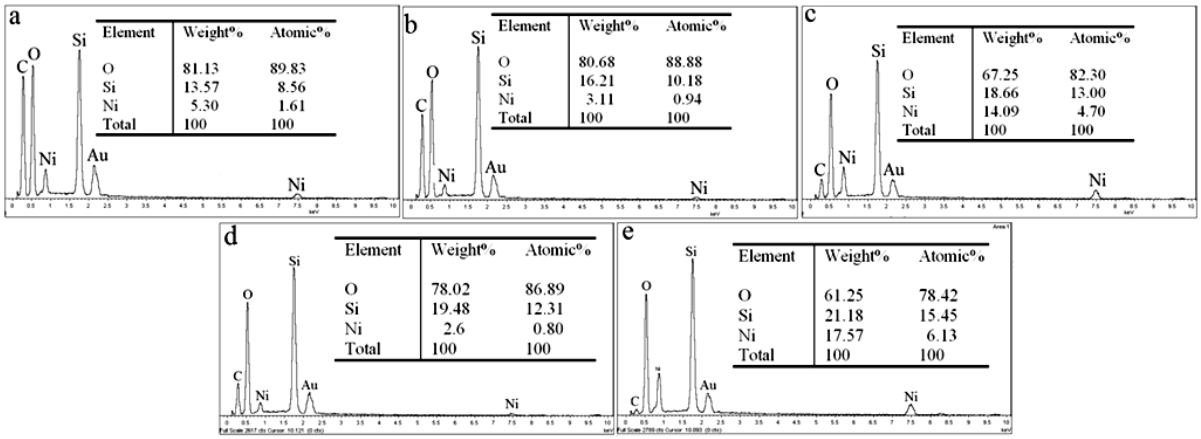

Fig. 6 EDX analysis results for chemical compositions of (a): NiMCF(9.2T-2D)(R), (b): NiMCF(12.5T-2D)(R), (c): NiMCF(16T-2D)(R), (d): NiMCF(9.2T-1D)(R) and (e): NiMCF(9.2T-3D)(R) catalysts

Table 4 Reaction results of solventless deoxygenation of palmitic acid over nickel functionalized MCF catalysts at 300 ^{o}C for 6 h.

Catalysts	Palmitic acid conversion, %	n-Pentadecane selectivity, %	1-Pentadecene selectivity, %
NiMCF(9.2T-2D)(R)	59.0	22	23.4
NiMCF(12.5T-2D)(R)	3.1	45	42.5
NiMCF(16T-2D)(R)	33.4	16	17.5
NiMCF(9.2T-1D)(R)	52.0	21	21.7
NiMCF(9.2T-3D)(R)	86.4	31.8	29.2

Furthermore, Table 4. also shows that selectivities of n-pentadecane performed by NiMCF(9.2T-2D)(R), NiMCF(16T-2D)(R) and NiMCF(9.2T-1D)(R) catalysts were a bit lower than those of 1-pentadecene in the palmitic acid deoxygenation. This result suggests that palmitic acid deoxygenation through decarboxylation was less selective than that through decarbonilation. On the other hand, palmitic acid deoxygenation over NiMCF(12.5T-2D)(R) and NiMCF(9.2T-3D)(R) catalysts gave a bit higher n-pentadecane selectivity compared to 1-pentadecane as the deoxygenation through decarboxylation was more intense than that through decarbonilation.

4. Conclusions

Preparation of MCF silica supports with different characteristics by varying TEOS amount and aging time was successfully carried out. With the same aging time in the MCF preparation, the increase in TEOS amount resulted in an increase in total surface area but its pore volume, cell size and window pore size experienced decreases due to a higher formation of Si-O-Si linkages. Further increase in TEOS amount caused a detrimental effect to the formation of the mesostructure in the MCF as condensations of the silica network were interrupted. Meanwhile, with the same TEOS amount in MCF preparation, the increase in aging time resulted in an increase in window pores size in the MCF materials attributed to an increase in size of the silica composites.

Incorporation of nickel into MCF supports was carried out using deposition-precipitation and then reduction process. The morphology of nickel functionalized MCF catalyst was strongly influenced by the structural characteristics of the MCF silica supports. With the same aging time in the MCF preparation, the increase in TEOS amount resulted in an increase in size of nickel particles that were dispersed in MCF silica due to a higher density of silanol groups (Si-OH) that reacted with nickel complex during the deposition-precipitation process. Meanwhile, with the same TEOS amount in the MCF preparation, the increase in aging time seemed to decrease the size of nickel particles dispersed in the catalysts but the amount of nickel content increased.

Among the MCF silica materials, MCF prepared using TEOS amount of 9.2 ml and aging time of 3 days MCF(9.2T-3D) was the most promising support for incorporation of nickel as the NiMCF(9.2T-3D)(R) catalyst obtained exhibited the highest palmitic acid conversion (86.4 %) with n-pentadecane selectivity of 31.8 % and 1-pentadecene selectivity of 29.2 % in solventless deoxygenation of palmitic acid at 300 ^{o}C under nitrogen flow for 6 h. The highest catalytic activity of NiMCF-9.2T(R) was attributed to the smallest nickel particle dispersed in the nickel functionalized MCF catalysts together with the highest nickel content (17.57 wt. %) as confirmed in SEM and EDX results

Acknowledgements A Research University (814181) grant from Universiti Sains Malaysia and aSciencefund (6013381) from MOSTI to support this research work are gratefully acknowledged. Lilis Hermida also thanks the Directorate General of Higher Education (DIKTI), Ministry of National Education of Indonesia for her PhD scholarship.

References

[1] Diesel will lead global fuel demand growth-OPEC. Available at**:** http://in.reuters.com/article/2009/07/08/opec-diesel-idINL859107920090708 Accessed November, 2012.
[2] Biomass. SJD Partner Limited-Sustainable energy provider page. Available at: http://www.sjdpartners.com/content/biomass Accessed January, 2013.
[3] Palm oil, available at: http://www.oilnfat.com/page0031.aspx Accessed January, 2013.
[4] Top AGM. Production and utilization of palm fatty acid distillate (PFAD). *Lipid Technology*. 2010; 22 (1):11-13.
[5] World's top producers target higher CPO output this year. Available at: http://biz.thestar.com.my/news/story.asp?%20file=/2012/1/20/business/20120120075710 Accessed January 2013
[6] Kikhtyanin OV, Rubanov AE, Ayupov AB, Echevsky GV. Hydroconversion of sunflower oil on Pd/SAPO-31 catalyst. *Fuel.* 2010;89:3085–3092.
[7] Lestari S, Arvela PM, Beltramini J, Lu GQM, Murzin DY.Transforming triglycerides and fatty acids into biofuels. *Chemistry & Sustainability*. 2009; 2:1109 – 1119.
[8] Identity and analysis of total petroleum hydrocarbon. Total petroleum hydrocarbon page. Available at: http://www.bvsde.paho.org/bvstox/i/fulltext/toxprofiles/total.pdf Accessed January, 2013.
[9] Snare M, Kubickova I, Ma1ki-Arvela P, Era1nen K, Yu D. Heterogeneous catalytic deoxygenation of stearic acid for production of biodiesel. *Industrial & Engineering Chemistry Research*. 2006;45:5708-5715.
[10] Lestari S, Ma1ki-Arvela P, Simakova I, Beltramini J, Max Lu G Q, Murzin DY. Catalytic deoxygenation of stearic Acid and palmitic acid in semibatch mode. *Catalysis Letter*. 2009;130:48–51.
[11] Na JG, Yi BE, Kim JN, Yi KB, Park SY, Park JH, Kim JN, Ko CH. Hydrocarbon production from decarboxylation of fatty acid without hydrogen. *Catalysis Today.* 2010;156;2010:44-48.
[12] Roh HS, Eum IH, Jeong DW, Yi BE, Nab JG, Ko CH. The effect of calcination temperature on the performance of Ni/MgO–Al_2O_3 catalysts for decarboxylation of oleic acid. *Catalysis Today*. 2011;164:457–460.
[13] Morgan T, Grubb D, Santillan-Jimenez E, Crocker M. Conversion of triglycerides to hydrocarbons over supported metal catalysts. *Topic in Catalysis*. 2010;53:820-829.
[14] Morgan T, Santillan-Jimenez E, Harman-Ware AE, Ji Y, Grubb D, Crocker M. Catalytic deoxygenation of triglycerides to hydrocarbons over supported nickel catalysts. *Chemical Engineering Journal.* 2012;189-190:346-355.
[15] Wilson K and Clark JH. Solid acids and their use as environmentally friendly catalysts in organic synthesis. *Pure and Applied Chemistry*. 2000;72:1313–1319.
[16] Perez-Pariente J, Diaz I, Mohino F, Satre E. Selective synthesis of monoglycerides by using functionalized mesoporous catalysts. *Applied Catalysis A: General*. 2003; 254:173- 188.
[17] Bossaert WD, Vos DED, Rhijn WMV, Bullen, J, Grobet, PJ, Jacobs PA. Mesoporous sulfonic acids as selective heterogeneous catalysts for the synthesis of monoglycerides. *Journal of Catalysis*. 1999;182:156–164.
[18] Schmidt-Winkel P, Lukens WW, Yang P, Margolese DL, Lettow JS, Ying JY, Stucky GD. Microemulsion templating of siliceous mesostructured cellular foams with well-defined ultralarge mesopores. *Chemistry of Materials*. 2000;12:686-696.
[19] Han Y, Lee SS, Ying JY. Siliceous mesocellular foam for high-performance liquid chromatography: Effect of morphology and pore structure, *Journal of Chromatography A*. 2010;1217:4337–4343.
[20] Nares R, Ramırez J., Gutierrez-Alejandre A., Cuevas R.,(2009). Characterization and hydrogenation activity of Ni/Si(Al)-MCM-41 catalysts prepared by deposition-precipitation. *Industrial & Engineering Chemistry Research*. 2009;48:1154–1162.
[21] Schmidt-Winkel P, Glinka CJ, Stucky GD. Microemulsion templates for mesoporous silica. *Langmuir*. 2000;16:356-361.
[22] Abdullah AZ, Kamaruddin AH, Razali N, Abdullah H, Bhatia S. Elucidation of interactive effects of synthesis conditions on the characteristics of mesoporous silicas templated using polyoxide surfactant, *Science and Technology of Advanced Materials*. 2007;8: 249–256.
[23] Louis C. Deposition-precipitation of supported metal catalysts. In: J.Regalbuto, Ed., *Catalyst Preparation Science and Engineering*. New York. Taylor and Francis; 2007:319-340.
[24] Hermida L, Abdullah AZ, Mohamed AR . Synthesis and characterization of mesostructured cellular foam (MCF) silica loaded with nickel nanoparticles as a novel catalyst. *Materials Sciences and Application*. 2013; 4:52-62
[25] Iler R (eds.). *The Chemistry of Silica*, New York: John Wiley & Sons; 1979.
[26] Sing KSW. Adsorption methods for the characterization of porous materials. *Advances in Colloid and Interface Science*.1998; 76-77:3-11.
[27] Na-Chiangmai C, Tiengchad N, Kittisakmontree P, Mekasuwandumrong O, Powell J, Panpranot J. Characteristics and catalytic properties of mesocellular foam silica supported Pd nano particles in the liquid-phase selective hydrogenation of phenylacetylene.*Catalysis Letters*. 2011;141(8):1149-1155.
[28] Kim J, Desch RJ, Thiel SW, Guliants VV, Pinto NG.Adsorption of biomolecules on mesostructured cellular foam silica: Effect of acid concentration and aging time in synthesis. *Microporous and Mesoporous Materials*. 2012;149(1):60-68.
[29] Hermida L, Abdullah AZ, Mohamed AR . Structure characteristics and catalytic activity of nickel supported on mesostructured cellular foam (MCF) silica for decarboxylation of palmitic acid: Effect of TEOS. *Proceedings of International Conference on Environmental Research and Technology*. Penang, Malaysia; 30 May-1 June 2012.
[30] Do DD. Adsorption science and technology. *Proceedings of the Second Pacific Basin Conference on Adsorption Science and Technology*, Singapore.World Scientific Publishing . Singapore; 2000.